Article

Spun-Up Rotation-Powered Magnetized White Dwarfs in Close Binaries as Possible Gamma-ray Sources: Signatures of Pulsed Modulation from AE Aquarii and AR Scorpii in Fermi-LAT Data

Pieter J. Meintjes *, Spencer T. Madzime, Quinton Kaplan and Hendrik J. van Heerden

Department of Physics, University of the Free State, Bloemfontein 9301, South Africa
* Correspondence: meintjpj@ufs.ac.za; Tel.: +27-51-401-2191

Abstract: In this paper, the possibility of periodic pulsar-like gamma-ray emission from the white dwarfs in AE Aquarii and AR Scorpii is investigated. We show that the white dwarf magnetospheres in AE Aquarii and AR Scorpii can possibly induce potentials to accelerate charged particles to energies in excess of one tera electronvolt (TeV) with associated gamma-ray emission through processes such as curvature radiation, inverse Compton, and hadronic processes such as neutral pion decay. We report here pulsed gamma-ray signatures at or close to the spin period of white dwarfs in both AE Aquarii and AR Scorpii in the Fermi-LAT dataset. This may indicate that both these white dwarfs possibly contain a particle accelerator that can produce relativistic electrons and ions and associated high energy radiation. The possibility of pair production is also investigated, which could provide a source for relativistic $e^{\pm}$ pairs in the magnetosphere. This could possibly be a driver for other forms of lepton-induced multi-wavelength pulsar-like emission from these two systems as well, for example, to explain the recently detected pulsed radio emission from AE Aquarii and R Scorpii in MeerKAT observations at the spin period of the white dwarf. The possibility of future detection of AE Aquarii and AR Scorpii with the Cherenkov Telescope Array (CTA) is also discussed. The future Vera Rubin Observatory will make a revolutionary contribution to time-domain astrophysics, which may lead to the discovery of thousands of new transient sources, possibly also many more close binaries with highly spun-up magnetized white dwarfs such as AE Aquarii and AR Scorpii for future investigation.

Keywords: white dwarf; pulsar; magnetic field; particle acceleration; gamma-ray emission; AE Aquarii; AR Scorpii

1. Introduction

The discovery of Cygnus X-3 as a very high energy (VHE) and ultra high energy (UHE) gamma-ray source in the 1980s, as well as similar reports related to Hercules X-1, 4U0115+63, and Vela X-1 (e.g., [1]) sparked enormous interest in the mechanisms responsible for particle acceleration and high energy gamma-ray production in accretion driven neutron star binaries. The acceleration of particles was believed to be based on a unipolar inductor process across the accretion disc [2] of an accreting neutron star. Soon after these initial discoveries, combined with the theoretical advances to develop models to explain particle acceleration and gamma-ray emission in disc accreting neutron star X-ray binaries (e.g., [3]), it has been shown that isolated highly magnetized white dwarfs with short rotation periods may also possess the necessary energetics to accelerate particles such as electrons and ions to high energies to produce VHE gamma rays through a variety of processes (e.g., [4,5]), of which some detail will be presented in the next section. Due to the fact that the underlying driving mechanism of the acceleration is based on the rotation power of a fast rotating, highly magnetized white dwarf, suitable candidates were searched for. Highly magnetized white dwarfs with short rotation periods can be produced via accretion torques (e.g., [6]) in close binary systems after periods of high mass transfer and accretion onto the white dwarf. For example, it was shown [7] that high

mass transfer episodes can occur in cataclysmic variables such as AE Aquarii, which can spin up the magnetic white dwarf over time scales as short as 10^4 years, far shorter than the thermal time scale ($\tau_{th} \sim 10^7$ years) of the mass donating star, which, under normal circumstances, drives the mass transfer process. For spun-up disc accreting white dwarfs, the unipolar inductor process (e.g., [2,3]) was initially believed to be instrumental for generating potentials to accelerate charged particles to VHE energies with associated VHE gamma-ray emission through a variety of processes.

　In light of these early developments, the first VHE studies of fast rotating, highly magnetized white dwarfs focused on the nova-like variable AE Aquarii in the 1980s–1990s. AE Aquarii's initial classification placed it in the DQ Hercules subclass of disc accreting magnetic cataclysmic variables containing a white dwarf rotating with a period of $P_* = 33.08$ s with a surface magnetic field probably in excess of $B_* \sim 10^6$ G at a distance of roughly d ~ 100 pc (e.g., [8]). The belief at that stage was that the system was a disc accretor, with the white dwarf being spun-up by accretion disc torques (e.g., [6]). However, later studies revealed that the optical pulsed signal strength is peculiarly low for a disc accretor [8] and that the rapid optical and radio variability can be reconciled with a fast rotating magnetic propeller that drives the mass transfer flow from the secondary star out of the binary system. This implies that the transient nature of the emission observed from AE Aquarii is not accretion driven but directly linked to the propeller ejection of mass from the system.

　Radio emission from observations with the VLA in the 1980s [9,10] was determined to be non-thermal and displayed rapid variability between 1 and 22 GHz. This was explained in terms of a superposition of synchrotron emission from expanding clouds of mildly relativistic electrons produced within the system. The rapid non-thermal radio variability resulted in AE Aquarii being classified as a low-power analogue of Cyg X-3 [10], which sparked enormous interest within the gamma-ray community in that period. Due to these physical properties and its close proximity, AE Aquarii was observed by different VHE groups in the 1980–1990s with telescopes spread across the United States (Whipple) (e.g., [11]), South Africa (Nooitgedacht) [12,13], and Australia (Narrabri) [14,15]. It was shown [12,13] that the nova-like variable AE Aquarii displays signatures of pulsed emission at energies $\epsilon_\gamma \sim 1$ TeV (Figure 1right) that resemble pulsed optical emission (Figure 1left) during flares.
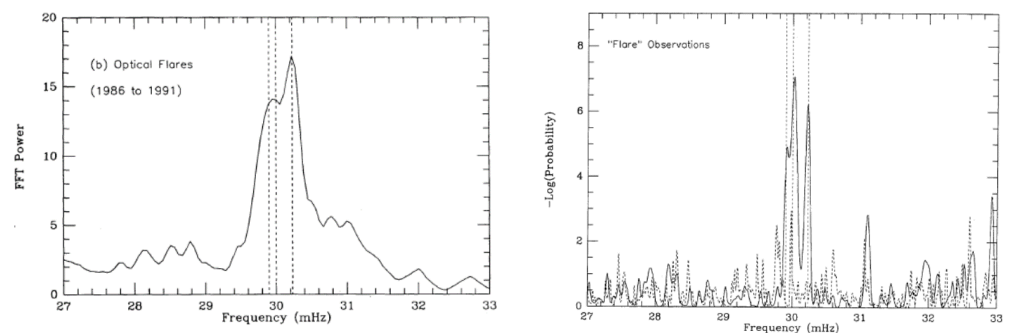

Figure 1. (**Left**) Pulsed optical emission detected during flares, typically at the spin frequency of the white dwarf with associated quasi-periodic emission at frequencies slightly shorter than the spin frequency. (**Right**) Pulsed VHE gamma-ray emission resembling the optical emission, usually detected during flares (Figures 1b and 9 from [12]).

　These features were consistently observed in the VHE gamma-ray observations of AE Aquarii resulting in the cumulative significance to increase steadily with time (see Figure 2) when the power spectra were stacked incoherently. The technique of stacking power spectra is useful to distinguish a low-level but consistent pulsed signal at a fixed frequency (or period) from the random white noise. It sums the power at a specific frequency in the respective periodograms (power spectra) to obtain a statistic that follows a χ^2 distribution with $2n$ degrees of freedom in the absence of a signal, where n represents the number of power spectra that were stacked [16].
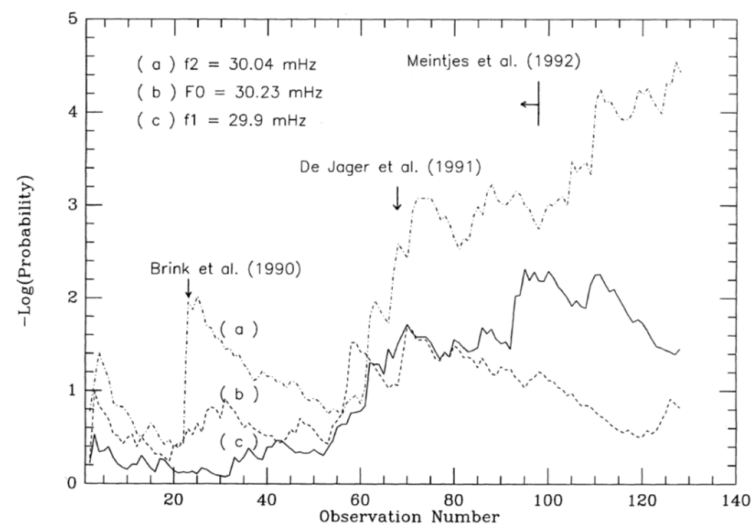
Figure 2. The cumulative significance of pulsed gamma-ray emission from AE Aquarii at frequencies usually seen during optical outbursts. The frequencies $f_1 = 29.9$ mHz, $f_2 = 30.04$ mHz are quasi periodic oscillations (QPOs) usually seen during optical flares, with $F_0 = 30.23$ mHz representing the spin frequency of the white dwarf (Figure 1 from [13]).

Contemporaneous studies in the 1980–1990s of AE Aquarii by the University of Durham's Very High Energy (VHE) group, with telescopes at Narrabri in Australia, revealed burst-like emission with associated pulsations in VHE at the 16.54 s (second harmonic) of the spin period (e.g., [14,15]). These burst-like events and associated pulsed emission were also confirmed during similar, but not simultaneous, events detected by the Nooitgedacht Cherenkov telescopes near Potchefstroom (South Africa) (e.g., [13]). The Nooitgedacht observations in the 1980s–1990s spanned 2 years with more than 200 h of data. However, the observations where a pulsed modulation was observed at the 33.03 s (or 16.54 s) periods implied a duty cycle of only a few percent.

These initial results, although very promising, were never confirmed by independent follow-up studies (e.g., [11] (*Whipple* telescope), [17,18] (*MAGIC* telescope)). The *MAGIC* observations resulted in no detection of any periodic signal above 2σ with only an upper limit above 200 GeV of $\sim6.4 \times 10^{-12}\,\mathrm{cm^{-2}s^{-1}}$, and above 1 TeV an upper limit of $\sim7.4 \times 10^{-13}\,\mathrm{cm^{-2}s^{-1}}$, assuming a Crab-like photon spectrum with a spectral index of $\Gamma = 2.6$ [18].

The recent optical-radio discovery of the close binary AR Scorpii [19–21], which contains a highly magnetized white dwarf emitting non-thermal radiation over a very wide frequency range, sparked renewed interest in spun-up white dwarfs as potential high energy sources (e.g., [22–26]). These observations showed that an important feature of this fascinating source is the interaction between a fast rotating magnetosphere of the white dwarf and the magnetic flux tubes of the secondary, which may be the driving force behind its enigmatic multi-wavelength emission (e.g., [22,23,25,26]). Optical spectroscopy [19] shows no indication that there is any mass transfer and accretion onto the surface of the white dwarf. This may imply that AR Scorpii, just like AE Aquarii, evolved through a high mass transfer phase that spun-up the white dwarf to a short rotation period of $P_* = 117$ s, after which the mass transfer from the secondary shut down, possibly due to nova eruptions or secondary star surface magnetic fields gating-off the mass flow across the L1 region. This implies that the white dwarfs in AE Aquarii and AR Scorpii are rotation powered in the current phase of their evolution.

It was recently shown [27] that the *Rotating Magnetic Vector Model* accounts for the white dwarf pulsar in AR Scorpii's position angle swings of the optical polarization reported by [23,24]. This further allows for well-constrained values of the magnetic obliquity and observer viewing direction with respect to the spin axis. These results suggest that the non-thermal emission arises from a dipolar magnetosphere close to the white dwarf star. These

authors continued to model the non-thermal emission geometry based on the constraints provided by phase-resolved polarimetry [28]. The last noted results firmly suggest that the dipolar magnetosphere of AR Scorpii is an active site of particle acceleration and possibly non-thermal synchrotron emission. Based on the fact that much of the non-thermal emission in AR Scorpii can be attributed to the interaction between the fast rotating magnetosphere of the white dwarf and the secondary star's magnetic field, [29] proposed a hadron channel for detectable high energy gamma-ray emission from AR Scorpii at energies above 1 GeV.

With *Fermi-LAT* [30] becoming operational in 2008, a new era dawned for the study of high energy emission in compact objects, especially after the Pass 8 data were released, which provide a better determination of the diffuse galactic gamma-ray emission as well as a significant improvement in the energy resolution from previous Fermi-LAT pipelines. Supplementary to this, the fact that the SKA precursor in South Africa, namely *MeerKAT* became operational, sparked renewed interest in sources that exhibit transient non-thermal multi-wavelength properties, among which are spun-up magnetized white dwarfs in close binary systems such as AE Aquarii and AR Scorpii.

The fact that rotation powered magnetized white dwarfs can be powerful cosmic accelerators has been theoretically established (e.g., [4,5,31–34]). These studies revealed that spin powered white dwarfs can be a new class of cosmic accelerator, which can accelerate charged particles to energies in excess of one TeV, which opens up the possibility of VHE gamma-ray emission through processes such as curvature radiation. Recent studies also attempted to establish a connection between the anomalous X-ray pulsars (AXPs)/soft gamma-ray repeaters (SGRs) and highly magnetized white dwarfs (e.g., [35,36]). However, it was shown (e.g., [37,38]) that both these classes (AXPs/SGRs) display observational properties that can be reconciled with magnetars, i.e., isolated neutron stars powered by magnetic energy. In the next section, a more detailed theoretical overview of particle acceleration in highly magnetized rotation powered white dwarfs will be presented. The discussion is focused specifically on the rotation powered white dwarfs in AE Aquarii and AR Scorpii, but can be extended to all rotation powered highly magnetized white dwarfs. The recent observational discovery of two more magnetized white dwarfs with short rotation periods (e.g., [39,40]), open up interesting possibilities for future investigation.

The paper is structured as follows: In the next section, a discussion of particle acceleration and associated gamma-ray emission in rotation powered white dwarf magnetospheres is presented. This is followed by a short summary of a recent *Fermi-LAT* search for pulsed gamma-ray emission from the spin powered white dwarfs AE Aquarii and AR Scorpii, respectively, with future prospects for follow-up studies utilizing the superior sensitivity and resolution of the Cherenkov Telescope Array (*CTA*). Concluding remarks are presented last.

2. Particle Acceleration and Non-Thermal Emission in White Dwarf Magnetospheres

The white dwarfs in AE Aquarii and AR Scorpii have possibly been spun-up in the past by accretion torques when the mass transfer from the secondary star was higher than it is currently. This results in both white dwarfs being in a phase presently where the transient multi-wavelength emission is not accretion driven but rather tied directly or indirectly to the rotation of a highly spun-up magnetized white dwarf. The basis for particle acceleration in these rotation powered systems will now be briefly discussed.

It can be shown (e.g., [41]) that electric and magnetic fields in a reference frame co-moving (primed quantities) with a highly conducting fluid or plasma can be expressed as

$$
\begin{aligned}
\mathbf{E}' &= \Gamma\left(\mathbf{E} + \frac{1}{c}(\mathbf{v} \times \mathbf{B})\right) \\
\mathbf{B}' &= \Gamma\left(\mathbf{B} - \frac{1}{c}(\mathbf{v} \times \mathbf{E})\right),
\end{aligned}
\tag{1}
$$

where $(\mathbf{E}'; \mathbf{B}')$, $(\mathbf{E}; \mathbf{B})$ represent the fields in the co-moving and laboratory frames, respectively, and Γ represents the bulk Lorentz factor. Here, $\mathbf{v}$ represents the relative velocity between the fluid (co-moving) frame and the stationary (laboratory) frame. For a highly

conducting fluid (i.e., $\sigma \to \infty$), the electric field in the co-moving frame $\mathbf{E}' \to \mathbf{0}$ and field quantities transform as follows to the laboratory, i.e., the observer's reference frame (un-primed quantities):

$$
\begin{aligned}
\mathbf{E} &= -\Gamma(\bar{\beta} \times \mathbf{B}') \\
\mathbf{B} &= \Gamma \mathbf{B}',
\end{aligned}
\tag{2}
$$

where $\bar{\beta} = \frac{\mathbf{v}}{c}$, and Γ represents the Lorentz factor. The maximum energy that can be attained by a charged particle of charge Ze is

$$
\begin{aligned}
\epsilon_{\max} &= Ze \int \mathbf{E}.\mathbf{ds} \\
&= q\beta\Gamma R_{\mathrm{s}} B',
\end{aligned}
\tag{3}
$$

where R_{s} and B' represent the size of the source and magnetic field in the frame of the source. In the fast rotating magnetosphere of a compact object such as a neutron star or a white dwarf, these velocity-related parameters (i.e., $\beta\Gamma$) are associated with the rotational velocity of the source with respect to a stationary observer. This expression clearly illustrates that for fast rotating compact objects satisfying ($\beta\Gamma >> 1$), the rotational kinetic energy reservoir relaxes the requirements for the strength of the intrinsic magnetic fields in the source to accelerate charged particles to high energies. The requirements regarding magnetic field and size of various classes of objects to accelerate protons and ions to energies in excess of $\epsilon_{\max} \sim 10^{20}$ eV (e.g., [34,42,43]) are displayed in Figure 3. Also shown (e.g., [34]) are the requirements of soft gamma-ray repeaters (SGRs) and anomalous X-ray pulsars (AXPs) to accelerate charged particles to these energies as either neutron stars (magnetars) or possibly highly magnetized white dwarfs with surface fields between 10^9 and 10^{12} G, which are extremely high for white dwarfs. Also included in Figure 3 are the magnetic requirements of AE Aquarii and AR Scorpii to accelerate charged particles to energies in excess of 10^{20} eV, revealing that both these white dwarfs should posses magnetic fields on the order of $>10^9$ G, which are very high for white dwarfs in close binaries.
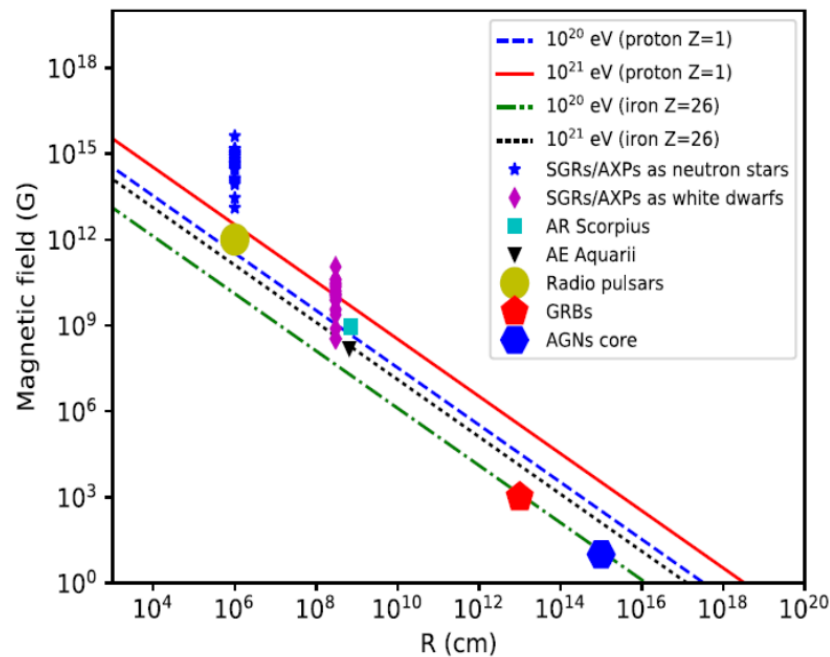

Figure 3. The Hillas diagram. On the horizontal axis there is the typical size of the source, and the vertical axis gives the typical source magnetic field. The diagonal lines correspond to the requirements for a 10^{20} eV and 10^{21} eV proton and heavy nucleus, respectively. The required magnetic field strength of the two sources AE Aquarii and AR Scorpii to accelerate charged particles to energies in excess of 10^{20} eV are $B' > 10^9$ Gauss, which is very high for white dwarfs (Figure 1 from [34]).

The two sources that we are focusing on in this study, i.e., AE Aquarii and AR Scorpii, are certainly among fast rotating white dwarfs in close binaries. Both these white dwarfs are currently in a spin-powered phase of their evolution and not accretion-powered like many white dwarfs in cataclysmic variables. The white dwarfs in both these objects are spinning down, i.e., $\dot{P} = 5.6 \times 10^{-14}\,\text{s s}^{-1}$ (AE Aquarii) (e.g., [44]), and $\dot{P} = 3.9 \times 10^{-13}\,\text{s s}^{-1}$ (AR Scorpii) [19].

Both white dwarfs in AE Aquarii and AR Scorpii display the same relationship between X-ray luminosity and spin-down power as is seen in most spin-powered pulsars, i.e., $L_X \sim 10^{-3} \dot{E}_{rot}$ (e.g., [45,46]) (see Figure 4), which, incidentally, is also similar to the requirement to explain the AXPs/SGRs as rotation powered white dwarfs (e.g., [36]). Both sources are not in an accretion phase of their evolution, e.g., AE Aquarii is a very effective magnetic propeller of mass from the system (e.g., [47–51]) resulting in an inferred propeller induced spin-down luminosity on the order of $L_{s-d} \sim 6 \times 10^{34}\,\text{erg s}^{-1}$ (e.g., [47,49,51]). It has been shown [49] that processes such as magnetic reconnection, which could be associated with the propeller process, may also drive particle acceleration and transient non-thermal emission.
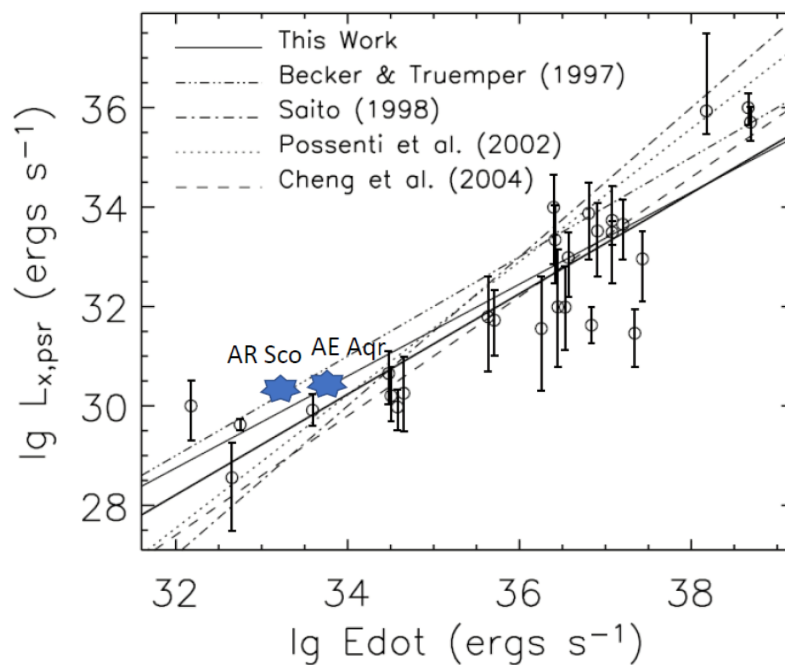

Figure 4. X-ray luminosity versus spin-down power of spin-powered neutron stars, compared to the white dwarfs in AR Scorpii and AE Aquarii. For AE Aquarii and AR Scorpii, the spin-down was measured by [19,44], respectively. These spin-down rates were used to estimate the spin-down power for these two sources respectively (e.g., [23,44]), (Figure 2 (adapted) with permission from [46]).

Spectroscopic observations reveal that AR Scorpii is not displaying any mass transfer from the secondary star and consequently no accretion [19]. The spin-down of the white dwarf in AR Scorpii is possibly due to a combination of a relativistic particle wind combined with a magnetospheric interaction with the secondary star (e.g., [23]) resulting in a spin-down luminosity on the order of $L_{s-d} \sim 1.5 \times 10^{33}\,\text{erg s}^{-1}$. Therefore, the conditions for particle acceleration in the magnetosphere of these two white dwarfs may be somewhat similar to the prevailing conditions in isolated neutron star magnetospheres, which are prolific accelerators of charged particles to energies in excess of 10^{11}–10^{12} eV (e.g., [52–54]).

Particle acceleration, specifically in the magnetospheres of magnetized white dwarfs, was considered in the late 1980s to early 1990s [4,5]. It was shown that, for non-accreting white dwarfs [4], the scale height of the white dwarf atmosphere is

$$H_s \approx \frac{kT_s R^2}{m_p G M_*} \sim 10^4 \left(\frac{R_*}{10^9 \text{ cm}}\right)^2 \left(\frac{M_*}{M_\odot}\right)^{-1} \left(\frac{T_s}{10^5 \text{ K}}\right) \text{ cm}, \tag{4}$$

which is several orders of magnitude smaller than the radius of the white dwarf and implies that above this zone the atmosphere essentially becomes a vacuum. The critical charged particle density for which electric fields can be sustained in the magnetosphere can be obtained from Gauss' equation (e.g., [52]), i.e.,

$$n_{GJ} = \frac{\mathbf{\Omega} \cdot \mathbf{B}}{2\pi e c} \approx 10^4 \, B_6 \Omega \text{ cm}^{-3}, \tag{5}$$

which implies that potentials can only exist in extremely tenuous regions of the white dwarf magnetosphere where charged particle densities $n < n_{GJ}$. For accreting white dwarfs, this condition will never be met, which rules out pulsar-like particle acceleration above the polar cap for these systems. However, the white dwarfs in AE Aquarii and AR Scorpii are not accreting, which may suggest that the particle density in the magnetosphere of these white dwarfs above one scale height from the surface on the polar cap may be sufficiently tenuous to sustain electric potentials to accelerate particles to high energies. Applying the basic ideas of [4,5], with modifications introduced by [55], to the white dwarf in AE Aquarii [56–58] and AR Scorpii [23,59,60], respectively, revealed that both these white dwarfs can indeed be sources of high energy particles and subsequent high energy gamma-ray emission. For example, it was shown for AE Aquarii [57], adopting the following parameters $P_* = 33.08$ s, $R_* \sim 10^9$ cm, $B_* \sim 10^6$ G, the potential between the surface of the white dwarf and the light cylinder, i.e., where the magnetosphere rotates with the velocity of light, scales as

$$V = \int_R^r E_{||} ds = 2 \times 10^{11} P_{33}^{-5/2} \mu_{33} R_9^{1/2} \left[\left(\frac{r}{R}\right)^{1/2} - 1 \right] \text{ V}. \tag{6}$$

It can then be shown that close to the light cylinder $r = r_L = \frac{c}{\Omega_*}$, the total potential will be on the order of

$$V(r_L) \approx 2 \times 10^{12} P_{33}^{-2} \mu_{33} \text{ V}, \tag{7}$$

which implies $\gamma_p(r_L) \sim 4 \times 10^6$. These estimates are based on a magnetic field intensity of $B_* \sim 10^6$ G, which may in fact be a lower limit on the surface field intensity [56].

Electrons accelerated close to the white dwarf will radiate their energy away in a characteristic time $\tau_{syn} \approx 8 \times 10^8 / (\gamma B^2)$ s [61] due to synchrotron radiation. This will result in these electrons losing the perpendicular component of their velocity relative to the magnetic field over a characteristic time scale τ_{syn}. Assuming a lower limit on the field strength of $B \sim 10^6$ G and Lorentz factors $\gamma \leq 10^6$, it can be shown for AE Aquarii as well as AR Scorpii that the characteristic synchrotron time scale near the surface of the star above the polar cap may be on the order of $\tau_s \leq 8 \times 10^{-10} \left(\frac{\gamma}{10^6}\right)^{-1} \left(\frac{B}{10^6 \text{ G}}\right)^{-2}$ s. As a result of the rapid radiation losses, the synchrotron channel will virtually immediately shut down close to the surface, and these electrons will glide down the curved field lines and emit curvature radiation with energy $\epsilon_c \sim \frac{\gamma^3}{R_c}$, where R_c represents the curvature radius of the magnetic field. However, energetic photons with energy exceeding $2m_e c^2$ in a strong magnetic field will produce pairs according to $\gamma + B \rightarrow e^+ + e^-$, which will be a very important opacity mechanism for high energy gamma-ray photons produced via curvature radiation close to the surface of the white dwarf [62,63].

The effect of magnetic pair production ($\gamma + B \rightarrow e^+ + e^-$) was first investigated in the polar cap regions above neutron stars (e.g., [64–67] with references therein) and white dwarfs (e.g., [63]). These authors showed that the region above the polar caps can be a site of $e^\pm$ production if high energy curvature radiated photons interact with the magnetic field to produce $e^\pm$ cascades under certain conditions. For a pure dipole field (e.g., [64,65]),

the average radius of curvature is $R_c \approx (R_* c / \Omega_*)^{1/2} \sim 5 \times 10^9 \left(\frac{R_{*,9}}{\Omega_*}\right)^{1/2}$ cm. However, these authors also noted that the radius of curvature can also be a factor ~ 100 smaller if multipoles contribute significantly to the field close to the surface. The threshold condition for $e^{\pm}$ production of a photon with energy $\epsilon_c = \hbar \omega_c \approx \gamma^3 \frac{\hbar c}{R_c}$ is (e.g., [31,33,53,62–65,68])

$$\left(\frac{\hbar \omega}{2 m_e c^2}\right)\left(\frac{B_\perp}{B_q}\right) = \gamma^3 \left(\frac{\hbar c / R_c}{2 m_e c^2}\right) \frac{B_\perp}{B_q} \approx \frac{1}{15}, \tag{8}$$

with $B_q = \frac{m_e^2 c^3}{e \hbar} = 4.4 \times 10^{13}$ G representing the quantum electrodynamic field, with $B_\perp = B_* \sin \theta$, and θ the angle between the direction of propagation of the photon with respect to the magnetic field lines, which may not necessarily be coincident with the dipole field. At a distance h above the surface, the $\sin \theta$ can be approximated with $\sin \theta \approx \frac{h}{R_c}$, resulting in $B_\perp \approx B_* \frac{h}{R_c}$ (e.g., [64,65]). Additionally, it was proposed [68] that positrons produced in these pair production reactions can be accelerated back to the surface of the white dwarf, which provides an interesting vehicle to explain pulsed X-ray emission in non-accreting fast rotating highly magnetic white dwarfs. This may well have implications for the white dwarfs in AE Aquarii and AR Scorpii, which show strong X-ray pulsations at the spin period of the white dwarf in the absence of accretion.

Keeping in mind that the electron energy $\gamma = \frac{e \Delta V}{m_e c^2}$, the threshold condition for pair production (e.g., [31,33,53,63–65,68]) is given by

$$\left(\frac{e \Delta V}{m_e c^2}\right)^3 \frac{\hbar}{2 m_e c R_c} \frac{h}{R_c} \frac{B_*}{B_q} \approx \frac{1}{15}, \tag{9}$$

where h represents the height of the accelerator zone above the polar cap of the white dwarf (not to be confused with $\hbar$). For the white dwarfs in AE Aquarii and AR Scorpii, we adopt surface magnetic field upper limits of $B_p \leq 100$ MG (e.g., [26,56]). Assuming a dipolar field topology, the maximum height of the accelerator gap is with $h_{max} = \frac{1}{\sqrt{2}} \left(\frac{R^3 \Omega}{c}\right)^{1/2}$ (e.g., [31,34,68]), which for AE Aquarii and AR Scorpii are

$$h_{max} \approx 5 \times 10^7 \left(\frac{R_*}{10^9 \text{ cm}}\right)^{3/2} \left(\frac{P_*}{33 \text{ sec}}\right)^{-1/2} \text{ cm} \quad \text{[AE Aquarii]} \tag{10}$$

$$h_{max} \approx 3 \times 10^7 \left(\frac{R_*}{10^9 \text{ cm}}\right)^{3/2} \left(\frac{P_*}{117 \text{ sec}}\right)^{-1/2} \text{ cm} \quad \text{[AR Scorpii]}. \tag{11}$$

If this value for the accelerator gap is adopted, the maximum potential difference of the accelerator is (e.g., [33,34,63,64,68])

$$\Delta V_{max} \approx \frac{B_* \Omega_*^2 R_*^3}{2 c^2}, \tag{12}$$

which results in values for the two sources under consideration

$$\Delta V_{max} \leq 6 \times 10^{14} \left(\frac{B_p}{10^8 \text{ G}}\right) \left(\frac{P_*}{33 \text{ sec}}\right)^{-2} \left(\frac{R_*}{10^9 \text{ cm}}\right)^3 \text{ Volt} \quad \text{[AE Aquarii]} \tag{13}$$

$$\Delta V_{max} \leq 5 \times 10^{13} \left(\frac{B_p}{10^8 \text{ G}}\right) \left(\frac{P_*}{117 \text{ sec}}\right)^{-2} \left(\frac{R_*}{10^9 \text{ cm}}\right)^3 \text{ Volt} \quad \text{[AR Scorpii]}. \tag{14}$$

With these assumptions, if we set $B_* \sim B_p$, the threshold condition for pair production is

$$\left(\frac{e\Delta V_{max}}{m_e c^2}\right)^3 \frac{\hbar}{2m_e c R_c} \frac{h_{max}}{R_c} \frac{B_p}{B_q} \approx \frac{1}{15}. \tag{15}$$

Introducing the expression for the potential difference according to Equations (13) (AE Aquarii) and (14) (AR Scorpii) and h_{max} according to Equations (10) and (11) into Equation (15) results in

$$\alpha = 3\log \Delta V_{max} + \log h_{max} - 2\log R_c + \log B_p \approx 33. \tag{16}$$

It can readily be shown that for the white dwarfs in AE Aquarii ($B_p \leq 10^8\,\text{G}$; $R_c \sim 1.14 \times 10^{10}\,\text{cm}$; $P_* \sim 33\,\text{s}$) and AR Scorpii ($B_p \leq 10^8\,\text{G}$; $R_c \sim 2 \times 10^{10}\,\text{cm}$; $P_* \sim 117\,\text{s}$), the condition specified in Equation (16) implies that for AE Aquarii ($\alpha \sim 33$) and AR Scorpii ($\alpha \sim 30$), respectively. These results seem to imply that, for the choice of parameters presented above, the threshold for magnetic pair production may be marginally satisfied for AE Aquarii, but perhaps not for AR Scorpii. Therefore, curvature photons produced close to the surface of the white dwarf may find the magnetosphere of AE Aquarii partially opaque, whereas it may be transparent for AR Scorpii. The possible magnetospheric pair production in AE Aquarii may have implications for pulsar-like radio emission from the white dwarf. Pulsed radio emission at the spin period of the white dwarf has been detected recently with the MeerKAT radio telescope in South Africa [69,70], which shows telltale signatures of synchrotron emission, which could possibly, in terms of the scenario described above, be related to the re-acceleration of pairs produced in the magnetosphere [69,70]. This is the first detection of pulsar-like pulsed radio emission at the 33.08 s spin period of the white dwarf in AE Aquarii. Pulsed radio emission has been detected from AR Scorpii [19–21] at a beat period between the white dwarf spin period and the orbital period of the system, which could be ascribed to magnetic pumping of the secondary star's magnetic field, rather than pure pulsar-like emission [19,23].

The curvature loss timescale (e.g., [71]) is given by $\tau_c \approx 180 R_c^2 \gamma^{-3}$, which will determine the maximum energy electrons can reach above the polar caps if curvature radiation is the dominant energy loss mechanism. If one assumes the acceleration time is proportional to the crossing time $\tau_{cross} \sim h_{max}/c$ of a relativistic particle, then the condition $\tau_c = \tau_{cross}$ will set the maximum energy. If for both these sources curvature radiation dominates the losses close to the surface of the white dwarf, the maximum electron energy will be on the order of

$$\gamma_{max} \approx \left(\frac{180 R_c^2 c}{h_{max}}\right)^{1/3}, \tag{17}$$

which implies that the maximum electron energy extracted from the accelerator is $\gamma_{max} \leq 2.4 \times 10^8$ (AE Aquarii) and $\gamma_{max} \leq 3.3 \times 10^8$ (AR Scorpii).

The typical curvature radiation energy (e.g., [34,64]) of photons is

$$\epsilon_c = \frac{3\hbar c \gamma^3}{2R_c} \tag{18}$$

resulting in the following upper limits for the two sources under consideration, i.e.,

$$\epsilon_c \leq 35 \left(\frac{\gamma}{2.4 \times 10^8}\right)^3 \left(\frac{R_c}{1.14 \times 10^{10}\,\text{cm}}\right)^{-1} \text{GeV} \quad [\text{AE Aquarii}] \tag{19}$$

$$\epsilon_c \leq 55 \left(\frac{\gamma}{3.3 \times 10^8}\right)^3 \left(\frac{R_c}{2 \times 10^{10}\,\text{cm}}\right)^{-1} \text{GeV} \quad [\text{AR Scorpii}] \tag{20}$$

near the surface of the white dwarf, which is within the Fermi-LAT energy window for both AE Aquarii and AR Scorpii.

Since the magnetosphere of AE Aquarii close to the white dwarf surface may be partially opaque to curvature photons, the pairs that are produced may well be accelerated further to achieve VHE energies with Lorentz factors in accordance with earlier estimates [57,58] to reach values $\gamma \to 10^6$, which may still allow a gamma-ray production channel via inverse Compton scattering. The contribution to the spectral energy distribution (SED) of both these systems as a result of synchrotron radiation and inverse Compton scattering will now be investigated.

Based on the model proposed by [4,5,55,56], it has been shown [57,58] that electrons accelerated in the electric fields parallel to the magnetopsheric field in AE Aquarii and AR Scorpii [23,60] close to the light cylinder could achieve energies of at least the order of $\gamma_e \sim 10^5 - 10^6$. If curvature radiation of relativistic electrons close to the light cylinder is possible, it may contribute significantly towards the SED in the optical and X-ray band, i.e., $\epsilon_c \sim 3 \left(\frac{\gamma}{10^5}\right)^3 \left(\frac{R_c}{10^{10}}\right)^{-1}$ eV–$3 \left(\frac{\gamma}{10^6}\right)^3 \left(\frac{R_c}{10^{10}}\right)^{-1}$ keV and may perhaps contribute to the possible power-law X-ray component reported by [72]. The possibility of gamma-ray emission through the synchrotron process in AR Scorpii was investigated [73]. These authors showed that synchrotron radiation alone from relativistic electrons in the white dwarf magnetosphere of AR Scorpii cannot replicate any part of the SED above 100 MeV but may contribute substantially towards the X-ray spectrum [26].

The possibility of a significant inverse Compton contribution to the gamma-ray SED above 100 MeV will depend on whether the scattering process occurs in the Thomson or Klein–Nishina (K-N) limit of the scattering cross section. If the acceleration mechanism in both these sources will produce a significant portion of electron-positrons with Lorentz factors of $\gamma_e \sim 10^6$ close to the light cylinder, the scattering will occur in the Thomson limit if there is a sufficient reservoir of target photons with energies below

$$\nu < \frac{m_e c^2}{\gamma_e h} < 10^{14} \left(\frac{\gamma_e}{10^6}\right)^{-1} \text{ Hz.} \tag{21}$$

The peak of the black body radiation field for K-type and M-type dwarf stars ($T_e \sim 3500$ K–4500 K) occurs at a frequency

$$\nu_{max} = \frac{2.82 k T_e}{h} \sim 10^{14} \left(\frac{T_e}{4000 \text{ K}}\right) \text{ Hz.} \tag{22}$$

Inverse Compton scattering between relativistic electrons and photons with frequency $\nu \geq 10^{14}$ Hz will probably occur in the K-N limit of the cross section and in the Thomson limit for $\nu \leq 10^{14}$ Hz. For both these sources, there should be a sufficient reservoir of photons with frequencies below the peak of the black body spectrum to act as targets for ultra-relativistic electrons to be upscattered to gamma-ray energies in the Thomson limit [58–60]. The maximum inverse Compton scattered gamma-ray energy for electron energies on the order of $\gamma \leq 10^6$ if we consider that there may be optical photons ($\epsilon_{phot} \sim 1$ eV) from the secondary star, or alternatively curvature radiation photons produced by pairs close to the light cylinder, will be on the order of

$$\epsilon_{IC,\gamma} \leq 4\gamma^2 \epsilon_{phot} \leq 4 \left(\frac{\gamma}{10^6}\right)^2 \left(\frac{\epsilon_{phot}}{1 \text{ eV}}\right) \text{ TeV,} \tag{23}$$

which provides an interesting possibility for high energy emission from both these sources.

The possibility of gamma-ray emission through both leptonic and hadronic channels was considered from the close binary AR Scorpii [29]. Based on the fact that efficient particle acceleration can occur due to the pumping of the magnetosphere of the secondary star by the fast rotating white dwarf [22,23,25], $e^{\pm}$-pairs can be created as a result of the decay of charged pions ($p + p \to \pi^{\pm} \to e^{\pm}$), which can produce detectable non-thermal emission in the X-ray band, explaining the *Swift* X-ray spectrum (e.g., [26]), whereas high energy gamma-rays can be produced through the channel $p + p \to \pi^{\circ} \to 2\gamma$ that can possibly be detected by *Fermi-LAT*, *MAGIC*, *H.E.S.S*, and *CTA* at energies $\epsilon_{\gamma} > 10$ GeV [29].

The initial reports of VHE gamma-ray emission from AE Aquarii (e.g., [12–14]) can also be explained within the realm of hadronic acceleration and accompanying VHE emission through neutral pion decay. The presence of the secondary star as well as the reservoir of ejected material by the magnetic propeller process may provide sufficient target material for neutral pion production and subsequent gamma-ray emission.

From this discussion, it can be seen from an energetics perspective that high energy gamma-ray emission from the white dwarfs in both close binaries AE Aquarii and AR Scorpii is certainly a possibility through leptonic (curvature radiation and inverse Compton scattering) and hadronic channels (neutral pion decay). Because our calculations suggest the possibility of pulsed gamma-ray emission from both these sources that may be detectable in the Fermi-LAT energy window, we focused on the search for periodic gamma-ray emission from both these sources. Therefore, utilizing the long Fermi-LAT data baseline of more than a decade, using the Pass 8 dataset, a search for gamma-ray emission was conducted from both AE Aquarii and AR Scorpii.

3. Fermi-LAT Observations of AE Aquarii and AR Scorpii

The Fermi Gamma-ray Space Telescope was launched by NASA on 11 June 2008 into a low earth orbit (LEO) at an altitude of 550 km. The Large Area Telescope (LAT) is the primary instrument on the Fermi Gamma-ray Space Telescope, formerly known as the Gamma-ray Large Area Space Telescope (GLAST). *Fermi-LAT* is in constant survey mode, and covers the whole gamma-ray sky every 3 h. It has a large field of view of 2.4 sr at 1 GeV, about 20% of the sky. The corresponding energy sensitivity is between 0.1 and 500 GeV. The point spread function (PSF) is approximately 68% containment radius. Fermi-LAT data access, tutorials, and software tools can be accessed through the Fermi Science Support Center (https://fermi.gsfc.nasa.gov/ssc/, accessed on 28 December 2022). Pass 8 provides the new version of the LAT data, which is the improved version of the Pass 7 reprocessed data. The entire dataset of the mission is reprocessed, including the upgraded event reconstruction, a broader energy range, an increased effective area, and better energy measurements (e.g., [30]). Two essential fits files are extracted from the LAT data: the photon file and the spacecraft file. The photon file comprises information necessary for science analysis, such as the event's energy, the quality of the event reconstruction, and the position. On the other hand, the spacecraft file gives the information of where the LAT was pointing, i.e., it consists of the position of the spacecraft and corresponding time (in 30 s intervals) of its orientation. The LAT data also have an extended file, which has the same photon data as the photon file along with supplementary photons with more relaxed cuts. However, this file is normally not utilized during the standardized Fermi science tools processes.

3.1. AE Aquarii

The first Fermi-LAT search for gamma-ray emission from AE Aquarii used a data baseline of 7 years, with no detection of coherent pulsations above 3σ with only an upper limit on the gamma-ray flux of reported of $\sim 1.3 \times 10^{-12}$ erg cm^{-2}s^{-1} [74]. In the present study, the Fermi-LAT archived gamma-ray data observed between 2008-08-04 at 15:43:36 and 2020-03-25 at 05:21:17 were considered, i.e., a data baseline of roughly 12 years. The analysis was undertaken using the Fermi Science Tools software packages (v11r0p5) installed with Anaconda python package. We used the P8R3-SOURCE-V2-v1 set of response functions and selected corresponding source-lass events, event class (evclass = 128) and FRONT+BACK event type (evtype = 3). Analysis photons were collected from a 10 degree region of interest (ROI) with its center at AE Aquarii (RA = 310.038°, DEC = −0.8708° epoch J2000), which was chosen to account for the PSF of the LAT instrument. The zenith angle cut was set at 90° to prevent contamination by photons produced from cosmic-ray interaction with the atmosphere. Binned and unbinned maximum likelihood analyses were performed on the energy range 0.1–500 GeV using the gtlike/pyLikelihood routine. Sources within 20° of the ROI from the fourth catalogue of *Fermi-LAT* (4FGL), the instrumental background,

and the diffuse galactic and extragalactic isotropic emission model (gl-iem-v07.fits), as well as the source of interest, were included in the spectral model file. The analysis of AE Aquarii was undertaken making use of a power law and the spectral model for pulsars, i.e., a power law with the exponential-cutoff2. The search for steady gamma-ray emission was conducted using binned and unbinned standard analysis utilizing the upgraded Fermi-LAT Pass 8 dataset. The search for periodic modulation of gamma-ray emission was conducted using the *gtpsearch* and *gtpphase* routines of the Fermi Science Tools software packages.

Utilizing the full 12 year Pass 8 dataset with standard Fermi-tools revealed no significant steady emission above the 2σ level [70] from AE Aquarii ($\sigma = \sqrt{TS}$, [75]. A large value of TS implies a rejection of the null hypothesis.

The unbinned and binned (see [70], pp. 67–68 for a detailed discussion) gamma-ray spectra associated with data sections that display a significance above 1σ were produced (see Figure 5a(top, left panel)). Both spectra display a clear power-law profile with photon index $\Gamma \sim 2$. Also shown in Figure 5a(top, right panel) is that the gamma-ray flux for both binned and unbinned analysis seems to be more concentrated in the energy bins below $\sim$ 5 GeV. Repeating this same analysis [69,70] in data sections showing higher significance ($\geq 2\sigma$), which may imply higher level gamma-ray activity than usual, evidence of spectral hardening is detected (see Figure 5b(bottom, red spectrum)). This certainly seems to suggest that AE Aquarii may be of interest for more sensitive Air Cherenkov detectors like *CTA*, especially during periods of higher level activity, such as possible flares.

When a light curve was determined for AE Aquarii, there were sections in the light curve that revealed gamma-ray emission above the 2σ significance level [69,70]. Focusing on these data sections, breaking it up in 10 min sections, each section was searched for periodicity. The periodograms of these sections all had the same frequency resolution, and were then added (stacked) incoherently [69,70]. These stacked power spectra reveal clear indications of pulsations at both 33.08 s and 16.54 s periods (see Figure 6a(left) for a few examples). (See [70] for a more detailed discussion with a complete set of power spectra.) To test whether these pulsations are not spurious, we selected regions in the sky consecutively further away from AE Aquarii's position in the sky 3°–15° and produced the same power spectra for the same periods. From Figure 6a, one can see a gradual weakening of the pulsed power at the 33.08 s and 16.54 s in regions further away from AE Aquarii's position in the sky.

The number distribution of the Rayleigh test statistic $\log(dN/dZ)$ vs. Z, with Z representing the Rayleigh rest statistic ($Z = 2nR^2$) [76], which quantifies the pulsed power, has been plotted in the frequency interval that was analyzed for periodicity. This distribution for a pure white noise profile will follow an inverse linear trend in the power distribution. Any deviation in the linear trend signifies a deviation of pulsed power from a pure white noise profile and may indicate the possible presence of a periodic modulation in the data. The distributions ($\log(dN/dZ)$ vs. Z) in the frequency range presented in Figure 6a have been determined and presented in Figure 6b(right). The power spectrum that correlates with AE Aquarii's position in the sky shows a clear deviation of the distribution of pulsed power from the white noise linear fit (blue line), which signifies that the distribution of Rayleigh power does not conform to a white noise distribution in the frequency range under consideration. However, one can see from Figure 6b that the distribution of Rayleigh power conforms to white noise in the power spectra that were taken consecutively further away from AE Aquarii's position in the sky 3°–15°, which is to be expected since no periodic signal associated with AE Aquarii is expected outside the Fermi-LAT point source window, which is approximately 2°. This also correlates with the fact that pulsed power at the 33.08 s and 16.54 s periods associated with AE Aquarii gradually decreases in the power spectra further away from AE Aquarii's position in the sky (Figure 6a).
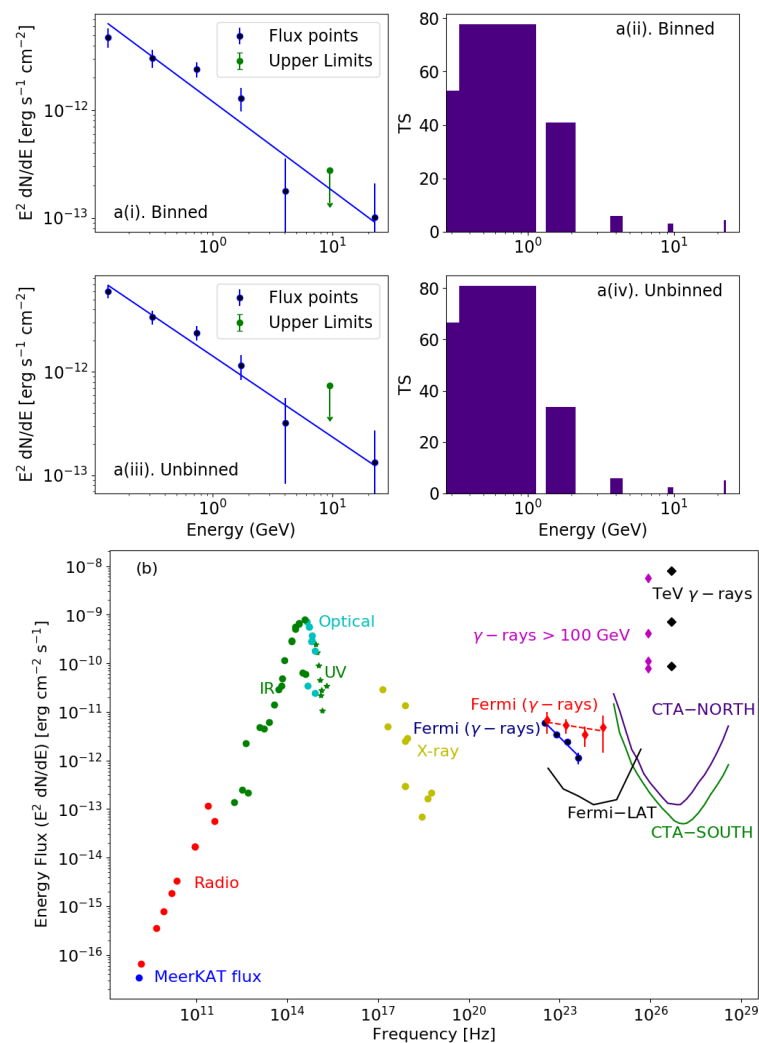
Figure 5. (**a**, top left panel) Gamma-ray spectra for both binned and unbinned analysis showing power-law profiles with photon index $\Gamma \sim 2$. (**a**, top right panel) Both analyses show that the flux is concentrated in the energy bins below ~ 5 GeV. (**b**, bottom) The SED for AE Aquarii, showing the gamma-ray spectra for quiescence (blue) and flare (red) sections of the Fermi-LAT data. Spectral hardening is visible (red spectrum), which may suggest that AE Aquarii could be of interest for Cherenkov Telescope Array (CTA) follow-up studies. (Adopted from [70], M.Sc dissertation, University for the Free State.)

Fermi-LAT data sections that coincide with optical flares observed with the UFS-Boyden 1.5 m telescope were selected for periodic analysis [70].

Individual power spectra corresponding to flares have been established with the same resolution to enable incoherent stacking (see Figure 7a(left)). It is clear from Figure 7a that the gamma-ray periodograms coinciding with enhanced optical activity show a pulsed modulation at a period that corresponds to the spin period of the white dwarf. This analysis confirms earlier reports of a 33 s pulsed modulation during epochs that coincide with optical flares (e.g., Figure 7b(right)).
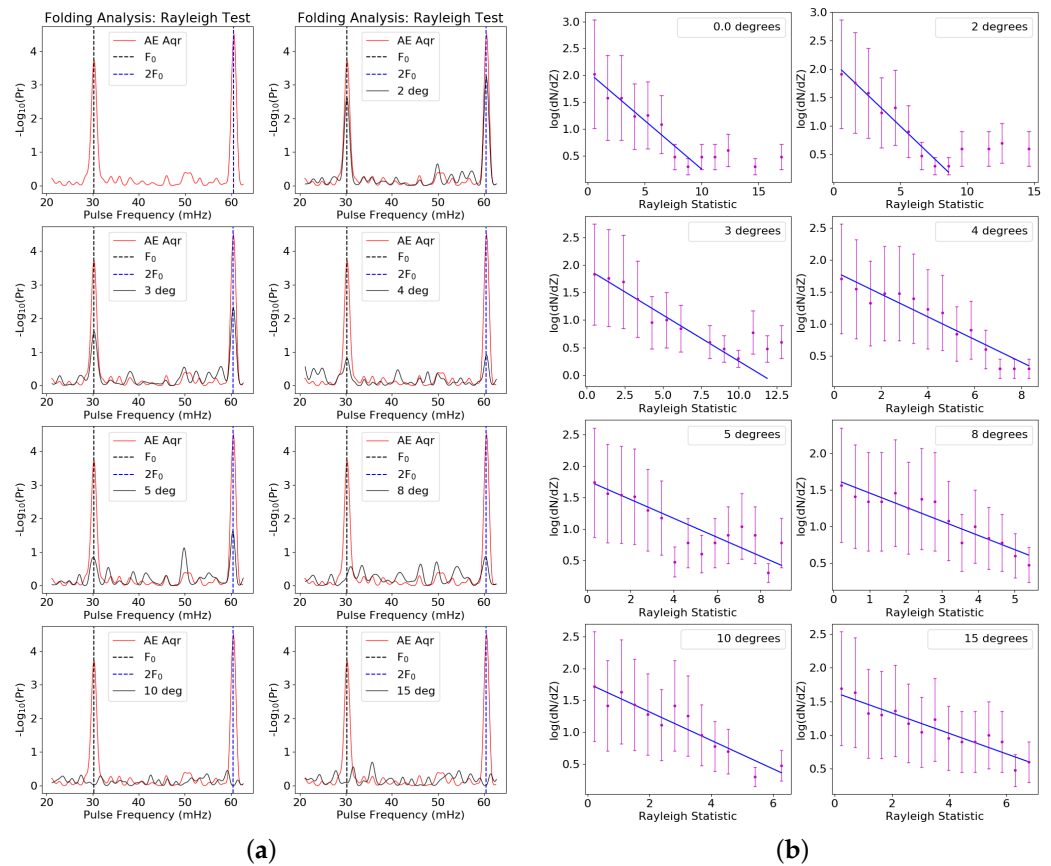
Figure 6. (**a**) Example of stacked Fermi power spectra of AE Aquarii of epochs showing gamma-ray emission above the 3σ significance level. Clearly visible is the decrease in pulsed power at $F_\circ$ and $2F_\circ$ further away from AE Aquarii's position in the sky. (**b**) Our control analysis shows how the differential number distribution of the Rayleigh statistic returns to a white noise distribution (blue solid line) further away from the source. This illustrates that the pulsed power is confined to AE Aquarii's position in the sky. (Adopted from [70], M.Sc dissertation, University of the Free State.)

A detailed investigation of the correlation between significant pulsed gamma-ray emission and the optical flares [70] seems to indicate that the strongest gamma-ray pulsed modulation is usually seen in the data sections just prior to optical flares: a phenomenon also observed during earlier studies in the late 1980s–1990s [13]. This can possibly be attributed to the fact that magnetospheric particle acceleration could be associated with the formation of double layers in the stressed magnetic fields due to the magnetospheric propeller effect, which could accelerate proton and electron beams to very high energy (VHE) with associated gamma-ray production via both leptonic and hadronic channels (see, e.g., [13,49]). This seems to imply that gamma-ray emission may not be exactly tied to the optical flare itself, which is caused by collisions between ejected plasma and associated radiative cooling, but rather to the severely distorted magnetospheric topology preceeding the flare when this plasma is ejected from the binary system (e.g., [47–49,51]).
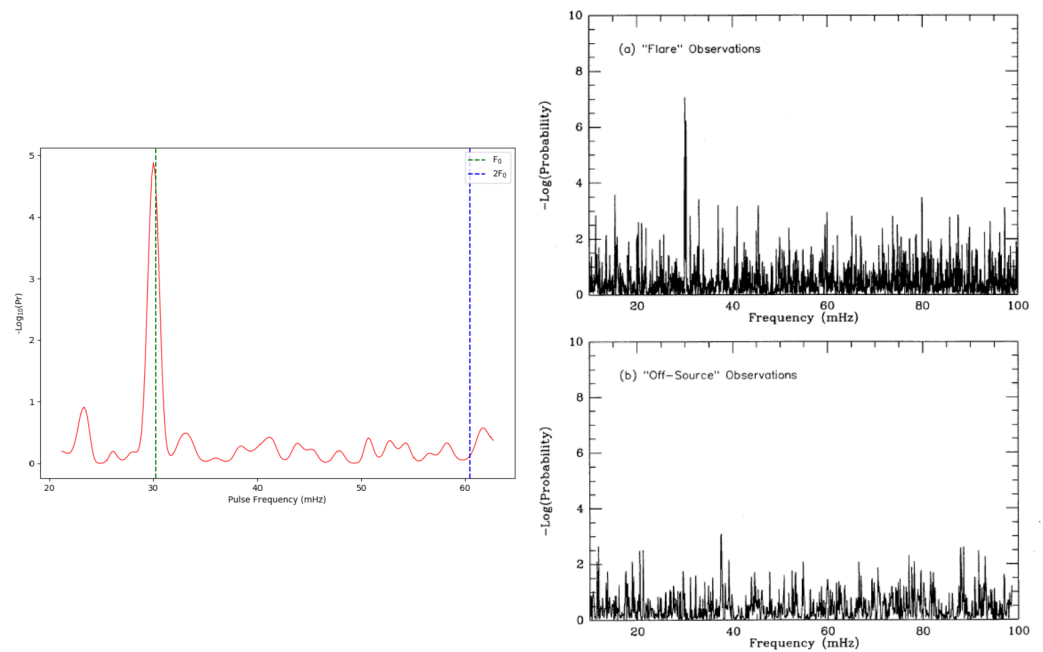
Figure 7. (**a**, left) Example of stacked Fermi-LAT power spectra of AE Aquarii during epochs that coincide with optical flaring observed by the UFS-Boyden 1.5 m telescope during three observational runs between 2010 and 2011 (adopted from [70], M.Sc dissertation, University of the Free State). (**b**, right) Reported VHE gamma-ray emission during periods that coincide with optical flaring during the 1980–1990s (Figure 7 from [12]).

3.2. AR Scorpii

Pass 8 Release 3 (P8R3) *Fermi*-LAT data from the past decade (4 August 2008–18 March 2019) were extracted from the Fermi Science Support Center (FSSC) in the energy range of 100 MeV to 500 GeV within a region of interest (ROI) of $10°$ centered at AR Scorpii (RA: $16^h21^m47.28^s$, Dec: $-22°53'10.39''$, J2000). Standard binned and unbinned likelihood analyses were performed using the recently released Fermi Tools software, *Fermi* 1.0.1. All the point sources in the fourth *Fermi*-LAT catalogue (4FGL) located within the ROI, along with recent galactic diffuse and extragalactic isotropic background emission models, were used to generate a background model for subtraction, keeping their spectral shapes the same as defined in the 4FGL catalogue. As AR Scorpii is not listed in the 4FGL catalogue, the methodology by manually adding the source to the model centered at its coordinates was used, parameterizing it with a power law spectral shape at first. The associated parameters of spectral models of all point sources within a $2°$ radius were chosen to be free to vary while performing the likelihood fitting.

After the likelihood analysis was performed, a SED was plotted using, e.g., the power law model over nine energy bins (see Figure 8 top). The SED was obtained using the *Fermi* build-in function `bdlikeSED` with the binned likelihood results. The energy flux values can be considered as 2σ upper limits based on a limiting TS < 4 value per bin due to the low overall significance of AR Scorpii. The distribution of TS values per energy bin (see Figure 8 bottom) also illustrates that the most significant emission is concentrated in the energy bins below 3 GeV. Due to *Fermi's* low spatial resolution at lower energies, it may be possible for other nearby sources, such as the strong gamma-ray quasar PKS1622-253, to contaminate the data associated with AR Scorpii's position in the sky.
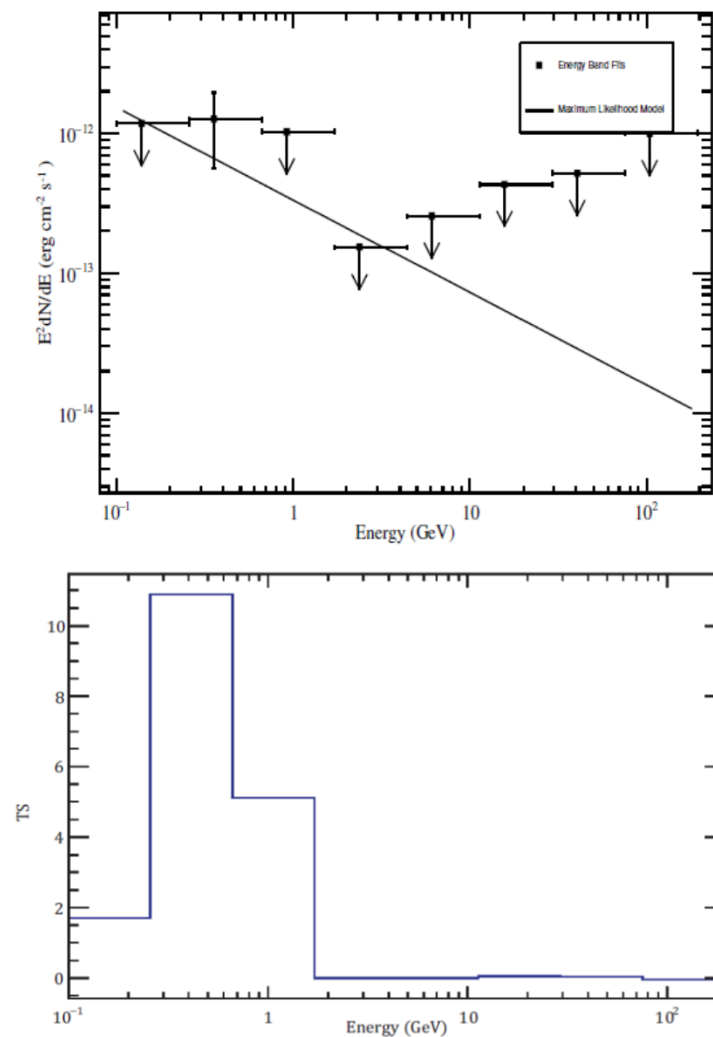
Figure 8. (**Top**) The flux values are 2σ upper limits. Distribution of high energy gamma-rays are more likely to be detected at lower energies. (**Bottom**) TS values vs. energy of gamma-ray photons indicate that the flux is mainly concentrated at energies below 1 GeV. (Adopted from [77], M.Sc dissertation, University of the Free State.)

No significant steady gamma-ray emission could be distinguished above the 2σ Fermi-LAT threshold (see Figure 9). A search for pulsed emission was conducted using the full 10 years Fermi-LAT data [77,78]. The power spectrum (Figure 10a) reveals a pulsed modulation at or close to the spin period of the white dwarf. The differential number distribution of the Rayleigh test statistic in the same frequency band shows a marginal deviation from a white noise distribution (Figure 10b), which may indicate the presence of low level pulsed gamma-ray modulation from AR Scorpii's position in the sky (see [77,78] for a more detailed discussion).

To test the validity of these results, regions in the sky further away from the position of AR Scorpii were selected and the same periodic analyses were conducted on those sections that were presented in Figure 10a,b. These control power spectra correspond to regions in the sky separated from the position of AR Scorpii between 2° and 8° are also shown in Figure 11left and Figure 11right). No significant pulsed emission at or close to the spin period of the white dwarf was detected, supported by the fact that the distribution of the Rayleigh test in these off-source regions conform to white noise. This may support the notion that low-level pulsed gamma-ray activity may in fact be associated with AR Scorpii, albeit statistically at a low significance level.
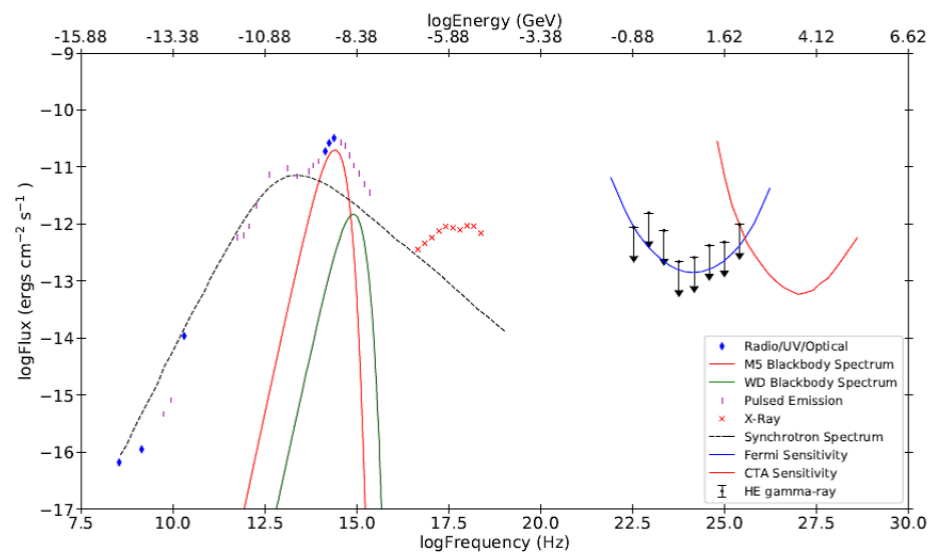
Figure 9. Gamma-ray spectrum combined with the multi-wavelength SED for AR Scorpii showing 2σ *Fermi-LAT* upper limits. No steady emission above 2σ could be discerned from the data. (Adopted from [77], M.Sc dissertation, University of the Free State.)
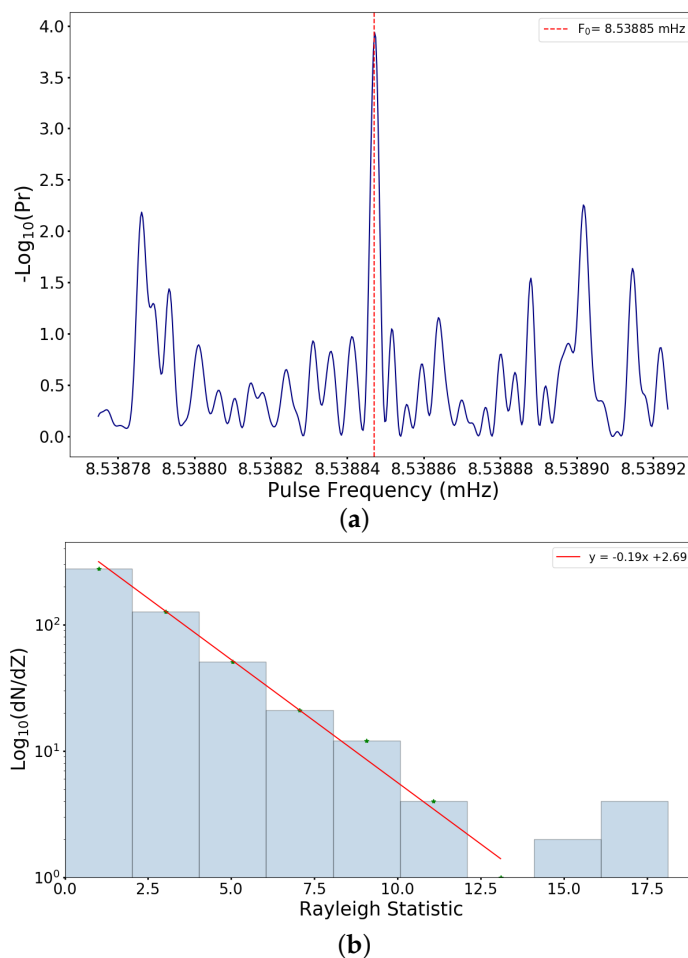

(a)

(b)

Figure 10. (**a**) The 10 year Fermi-LAT gamma-ray power spectrum revealing pulsations close to the spin period of the white dwarf in AR Scorpii. (**b**) The differential number distribution of the Rayleigh statistic in the same frequency interval reveals a marginal deviation from a pure white noise distribution, represented by the red solid line, which may indicate the presence of low level pulsed gamma-ray modulation from AR Scorpii's position in the sky. (Adopted from [77], M.Sc dissertation, University of the Free State.)
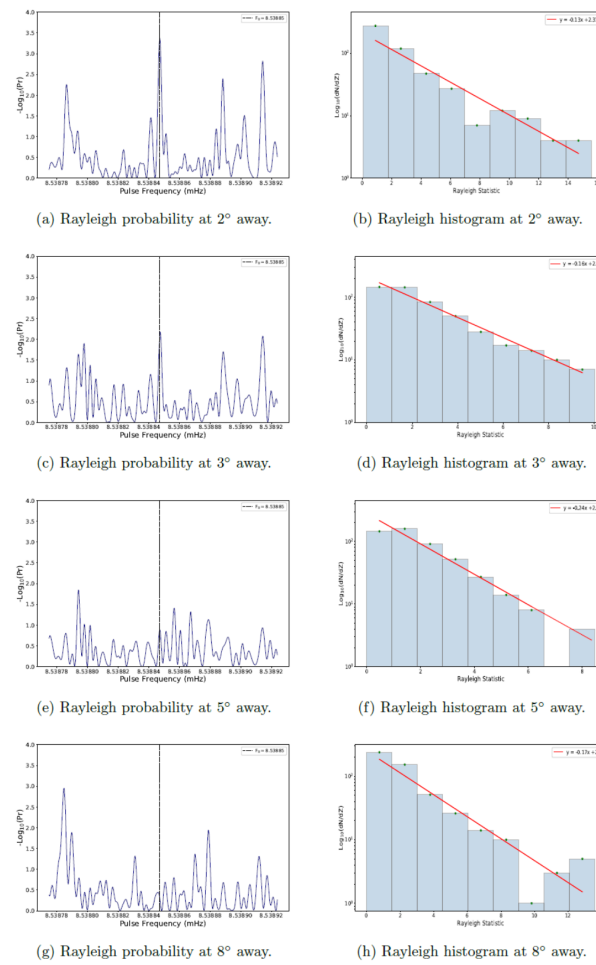
(a) Rayleigh probability at 2° away.

(b) Rayleigh histogram at 2° away.

(c) Rayleigh probability at 3° away.

(d) Rayleigh histogram at 3° away.

(e) Rayleigh probability at 5° away.

(f) Rayleigh histogram at 5° away.

(g) Rayleigh probability at 8° away.

(h) Rayleigh histogram at 8° away.

Figure 11. The left panel (**a,c,e,g**) represent power spectra from our control analysis where data were searched for periodic emission covering the same frequency interval as Figure 10 but in regions consecutively further away (2°–8°) from AR Scorpii's position in the sky. The right panel (**b,d,f,h**) represents the differential number distribution of the Rayleigh statistic of the periodograms presented in the left panel. The red solid line represents the fit corresponding to a pure white noise distribution. (Adopted from [77], M.Sc dissertation, University of the Free State.)

4. White Dwarf Pulsars in the CTA Era

The Cherenkov Telescope Array (CTA) will provide a paradigm shift in terms of sensitivity and angular resolution, combined with a wide field of view (fov) for rapid survey work. The CTA threshold energy for detecting atmospheric Cherenkov showers will overlap with the Fermi-LAT energy regime, which provides an unique opportunity for detailed combined studies of gamma-ray pulsar emission as well as potential gamma-ray burst (GRB) sources. Apart from detailed studies of neutron star pulsars, pulsar wind nebulae, and extragalactic sources such as blazars, the unique sensitivity of the CTA may provide the opportunity to study weaker emitters such as rotation powered magnetized white dwarfs. It has been shown (e.g., [31–36]) that these objects possess the required energetics to accelerate charged particles such as electrons and nuclei to relativistic energies, which may produce high energy gamma-ray emission through processes such as curvature radiation, inverse Compton scattering, and pion decay as a result of hadronic interactions. Based on the results presented in this study, the white dwarf pulsars AE Aquarii and AR Scorpii clearly possess the potential to accelerate charged particles to energies on the order of 1 TeV and higher, resulting in possible gamma-ray emission through a variety of processes that may be detectable with CTA. CTA has a huge potential over Fermi-LAT in the overlapping energy range for short transient phenomena in the field of view. This is clearly illustrated in Figure 12 when the energy flux sensitivity levels of CTA and Fermi-LAT are

compared [79]. CTA will reach the relevant flux levels for a 4–5σ detection for both AE Aquarii and AR Scorpii at energies $\epsilon_\gamma \leq 50$ GeV after observing times of $t_{obs} \sim$ few $\times 10^4$ s. However, it may be possible to extract a periodic signal after stacking power spectra of shorter observations with similar resolution. The confirmed detection of pulsed gamma-ray emission from both AE Aquarii and AR Scorpii may in fact establish isolated fast rotating highly magnetized white dwarfs as a new class of gamma-ray source and open up a whole new frontier in high energy astrophysics.
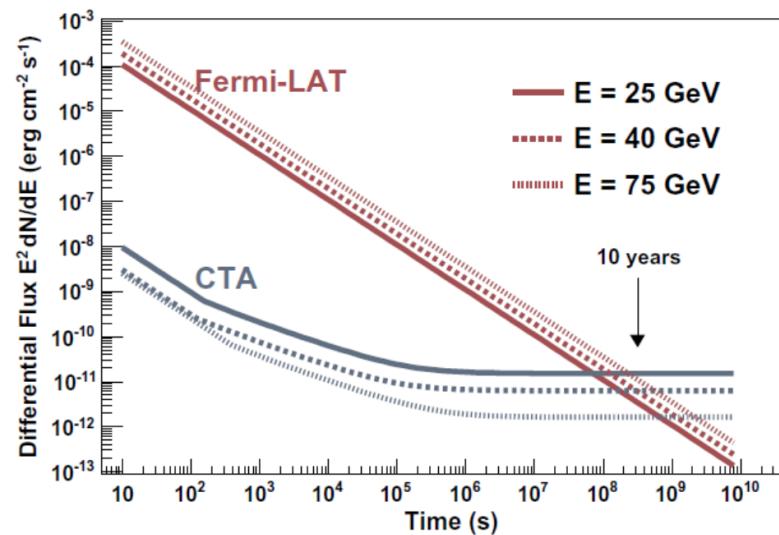
Figure 12. The differential flux sensitivity level *CTA* as a function of integration time compared with the *Fermi-LAT* 10 year sensitivity level at various energies. One can see that only after 10 years will *Fermi-LAT* reach comparable sensitivity at these energies (Figure 5 from [79]).

5. Conclusions

In this paper, the possibility of high energy emission from fast rotating white dwarf pulsars was evaluated based on the results of recent findings from two non-accreting fast rotating white dwarfs in close binaries, i.e., AE Aquarii and AR Scorpii [69,70,77,78]. It has been shown that, from an energy perspective, both white dwarfs in these systems may be the sites of particle acceleration and possible gamma-ray emission through both leptonic and hadronic channels. *Fermi-LAT* observations of both these systems over a time span of a decade showed indications of pulsed high energy gamma-ray modulation at, or slightly above, the Fermi-LAT threshold energy. AE Aquarii displays pulsed emission signatures similar to earlier reports of episodic and transient VHE gamma-ray events reported in the late 1980s–early 1990s by two independent groups. These reports, along with the latest Fermi-LAT results, seem to suggest that AE Aquarii could be a transient high energy source. The results from AR Scorpii are less convincing, but there seems to be a weak but constant pulsed modulation present in the data, which dissipates into the white noise further away from the source's position in the sky. The same phenomenon was observed with AE Aquarii. The superior sensitivity of CTA will provide new possibilities to study both these and possibly other similar sources. The results presented here, in conjunction with the theoretical discussion of particle acceleration in white dwarf magnetospheres, may suggest that fast rotating highly magnetic dwarfs could be a new class of cosmic accelerator and gamma-ray source, as has been suggested by, e.g., [31–36,43,63,68]. New possibilities to find observable sources will be created when the Vera Rubin Observatory (formerly the LSST) becomes operational. The Rubin Observatory [80] will use a 8.36 m aperture Simonyi Survey Telescope and its 9.6 deg^2 LSST camera to collect over 2 million sky images over a time span of 10 years. It will use multiple filters (*ugrizy*) with subarcsecond image quality, resulting in a $\sim$100 petabyte dataset after 10 year's observation. It will revolutionize time-domain astronomy by imaging the entire sky repeatedly in various energy bands every

night for 10 years. Any transient activity will create an alert upon which the astronomical community can respond with follow-up observations. It is anticipated that the Rubin telescope will create catalogues thousands of times larger than previous ones, which will perhaps result in the discovery of various new classes of transient sources that may be emitters in the high energy window as well.

References

1. Lamb, R.C.; Weekes, T.C. Very high energy gamma-ray binary stars. *Science* **1987**, *238*, 1528–1534. [CrossRef]
2. Chanmugam, G.; Brecher, K. Ultra-high energy gamma-rays and cosmic rays from accreting degenerate stars. *Nature* **1985**, *313*, 767–768. [CrossRef]
3. Cheng, K.S.; Ruderman, M. Period differences between X-ray and Very High Energy gamma-ray Observations of Accreting X-ray Pulsars. *Astrophys. J.* **1989**, *337*, L77–L79. [CrossRef]
4. Usov, V. Generation of gamma-rays by a rotating magnetized white dwarf. *Sov. Astron. Lett.* **1988**, *14*, 606–609.
5. Usov, V. High frequency emission of X-ray pulsar 1E 2259+586. *Astrophys. J.* **1993**, *410*, 761–763. [CrossRef]
6. Ghosh, P.; Lamb, F.K. Accretion by rotating magnetic neutron stars. III. Accretion torques and period changes in pulsating X-ray sources. *Astrophys. J.* **1979**, *234*, 296–316. [CrossRef]
7. Meintjes, P.J. On the evolution of the nova-like variable AE Aquarii. *Mon. Not. R. Astron. Soc.* **2002**, *336*, 265–275. [CrossRef]
8. Patterson, J. Rapid oscillations in Cataclysmic Variables III An oblique rotator in AE Aquarii. *Astrophys. J.* **1979**, *234*, 978–992. [CrossRef]
9. Bookbinder, J.A.; Lamb, D.Q. Discovery of radio emission from AE Aquarii. *Astrophys. J.* **1987**, *323*, L131–L135. [CrossRef]
10. Bastian, T.S.; Dulk, G.A.; Chanmugam, G. Radio flares from AE Aquarii: A low-power analog of Cyg X-3. *Astrophys. J.* **1988**, *324*, 431–440. [CrossRef]
11. Lang, M.J.; Buckley, J.H.; Carter-Lewis, D.A.; Catanese, M.; Cawley, M.F.; Colombo, E.; Connaughton, V.; Fegan, D.J.; Finley, J.P.; Gaidos, J.A.; et al. A search for TeV emission from AE Aquarii. *Astropart. Phys.* **1998**, *9*, 203–211. [CrossRef]
12. Meintjes, P.J.; Raubenheimer, B.C.; de Jager, O.C.; Brink, C.; Nel, H.I.; van Urk, G.; Visser, B. AE Aquarii: An emitter of pulsed gamma-ray emission resembling optical emission during flares. *Astrophys. J.* **1992**, *401*, 325–336. [CrossRef]
13. Meintjes, P.J.; de Jager, O.C.; Raubenheimer, B.C.; Nel, H.I.; North, A.R.; Buckley, D.A.H.; Koen, C. Simultaneous optical and TeV gamma-ray emission detected from AE Aquarii. *Astrophys. J.* **1994**, *434*, 292–305. [CrossRef]
14. Bowden, C.C.G.; Bradbury, S.M.; Chadwick, P.M.; Dickinson, J.E.; Dipper, N.A.; Edwards, P.J.; Lincoln, E.W.; McComb, T.J.L.; Orford, K.J.; Rayner, S.M.; et al. 350 GeV gamma-rays from AE Aqr. *Astropart. Phys.* **1992**, *1*, 47–59. [CrossRef]
15. Chadwick, P.M.; Dickinson, J.E.; Dickinson, M.R.; Dipper, N.A.; Holder, J.; McComb, T.J.L.; Orford, K.J.; Rayner, S.M.; Roberts, I.D.; Roberts, M.D.; et al. A burst of pulsed gamma-rays from AE Aquarii. *Astropart. Phys.* **1995**, *4*, 99–111. [CrossRef]
16. Eadie, W.T.; Drijard, D.; James, F.E. *Statistical Methods in Experimental Physics*; North-Holland: Amsterdam, The Netherlands, 1971; 296p.
17. Sidro, N.; Cortina, J.; Mauche, C.W.; de Oña, E.; Rico, J.; On behalf of the MAGIC Collaboration. Observation of AE Aquarii with the MAGIC Telescope. In *Proceedings of the 30th International Cosmic Ray Conference*; Caballero, R., D'Olivo, J.C., Medina-Tanco, G., Nellen, L., Sánchez, F.A., Valdés-Galicia, J.F., Eds.; Universidad Nacional Autónoma de México: Mexico City, Mexico, 2008; Volume 2, (OG Part 1), pp. 715–718.

18. Aleksić, J.; Ansoldi, S.; Antonelli, L.A.; Antoranz, P.; Babic, A.; Bangale, P.; Barrio, J.A.; González, J.B.; Bednarek, W.; Bernardini, E.; et al. MAGIC search for VHE γ-ray emission from AE Aquarii in a multiwavelength context. *Astron. Astrophys.* **2014**, *568*, A109. [CrossRef]

19. Marsh, T.R.; Gänsicke, B.T.; Hümmerich, S.; Hambsch, F.-J.; Bernhard, K.; Lloyd, C.; Breedt, E.; Stanway, E.R.; Steeghs, D.T.; Parsons, S.G.; et al. A radio-pulsing white dwarf binary star. *Nature* **2016**, *537*, 374–377. [CrossRef]

20. Marcote, B.; Marsh, T.R.; Stanway, E.R.; Blamchard, J.M. Towards the origin of the radio emission in AR Scorpii, the first radio-pulsing white dwarf binary. *Astron. Astrophys.* **2017**, *601*, L7. [CrossRef]

21. Stanway, E.R.; Marsh, T.R.; Chote, P.; Gänsicke, B.; Steeghs, D.; Wheatly, P.J. VLA radio observations of AR Scorpii. *Astron. Astrophys.* **2018**, *611*, A66. [CrossRef]

22. Geng, J.-J.; Zhang, B.; Huang, Y.-F. A model of white dwarf pulsar AR Scorpii. *Astrophys. J. Lett.* **2016**, *831*, L10. [CrossRef]

23. Buckley, D.A.H.; Meintjes, P.J.; Potter, S.B.; Marsh, T.R.; Gänsicke, B.T. Polarimetric evidence of a white dwarf pulsar in the binary AR Scorpii. *Nature Astron.* **2017**, *1*, 29. [CrossRef]

24. Buckley, D.A.H.; Potter, S.B.; Meintjes, P.J.; Marsh, T.R.; Gänsicke, B.T. Polarimetric Evidence of the First White Dwarf Pulsar: The Binary System AR Scorpii. *Galaxies* **2018**, *6*, 14. [CrossRef]

25. Katz, J.I. AR Sco: A precessing white dwarf synchronar. *Astrophys. J.* **2017**, *835*, 150–154. [CrossRef]

26. Takata, J.; Hu, C.-P.; Lin, L.C.C.; Tam, P.H.T.; Pal, P.S.; Hui, C.Y.; Kong, A.K.H.; Cheng, K.S. A non-thermal pulsed X-ray emission from AR Scorpii. *Astrophys. J. Lett.* **2018**, *853*, 106–114. [CrossRef]

27. du Plessis, L.; Wadiasingh, Z.; Venter, C.; Harding, A.K. Constraining the emission geometry and mass of the white dwarf pulsar AR Sco using the rotating vector model. *Astrophys. J. Lett.* **2019**, *887*, 44–54. [CrossRef]

28. Du Plessis, L.; Venter, C.; Wadiasingh, Z.; Harding, A.K.; Buckley, D.A.H.; Potter, S.B.; Meintjes, P.J. Probing the non-thermal emission geometry of AR Sco via optical phase resolved polarimetry. *Mon. Not. R. Astron. Soc.* **2022**, *510*, 2998–3010. [CrossRef]

29. Bednarek, W. Hadronic model for non-thermal radiation from the binary AR Scorpii. *Mon. Not. R. Astron. Soc. Lett.* **2018**, *467*, L10–L14. [CrossRef]

30. Ackermann, M.; Ajello, M.; Albert, A.; Allafort, A.; Atwood, W.B.; Axelsson, M.; Baldini, L.; Ballet, J.; Barbiellini, G.; Bastieri, D.; et al. The fermi large area telescope: Event classification, instrument response functions and calibration. *Astrophys. J. Suppl. Ser.* **2012**, *203*, 4. [CrossRef]

31. Kashiyama, K.; Ioka, K.; Kawanaka, N. White dwarf pulsars as possible cosmic ray electron-positron factories. *Phys. Rev. D* **2011**, *83*, 023002. [CrossRef]

32. Lobato, R.V.; Coelho, J.; Malheiro, M. Particle acceleration and radio emission for SGRs/AXPs as white dwarf pulsars. *J. Phys. Conf. Ser.* **2015**, *630*, 012015. [CrossRef]

33. Lobato, R.V.; Coelho, J.G.; Malheiro, M. Radio pulsar deathlines to SGRs/AXPs and white dwarf pulsars. Proceedings of the Second *ICRANet* César Lattes Meeting. *AIP Conf. Proc.* **2015**, *1693*, 030003 . [CrossRef]

34. Lobato, R.V.; Coelho, J.G.; Malheiro, M. Ultra-high energy cosmic rays from white dwarf pulsars and the Hillas criterion. *J. Phys. Conf. Ser.* **2017**, *861*, 012005. [CrossRef]

35. Coelho, J.G.; Malheiro, M. Similarities of SGRs with low magnetic field and white dwarf pulsars. *Int. J. Mod. Phys. Conf. Ser.* **2012**, *18*, 96–100. [CrossRef]

36. Malheiro, M.; Rueda, J.; Ruffini, R. SGRs and AXPs as rotation-powered massive white dwarfs. *Publ. Astron. Soc. Jpn.* **2012**, *64*, 56-1–56-13. [CrossRef]

37. Kaspi, V.M. Soft gamma-ray repeaters and Anomalous X-ray pulsars: Together forever, in Proceedings of the Young Neutron Stars and their Environments. *IAU Symp.* **2004**, *218*, 231–238. [CrossRef]

38. Mereghetti, S. The strongest cosmic magnets: Soft gamma-ray repeaters and anomalous X-ray pulsars. *Astron. Astrophys. Rev.* **2008**, *15*, 225–287. [CrossRef]

39. Kilic, M.; Kosakowski, A.; Moss, A.G.; Bergeron, P.; Conly, A.A. An isolated white dwarf with a 70 s spin period. *Astrophys. J. Lett.* **2021**, *923*, L6. [CrossRef]

40. Caiazzo, I.; Burdge, K.B.; Fuller, J.; Heyl, J.; Kulkarni, S.R.; Prince, T.A.; Richer, H.B.; Schwab, J.; Andreoni, I.; Bellm, E.C.; et al. A highly magnetized and rapidly rotating white dwarf as small as the moon. *Nature* **2021**, *595*, 39. [CrossRef]

41. Jackson, J.D. *Classical Electrodynamics*, 2nd ed.; Wiley & Sons: New York, NY, USA, 1975; pp. 473–552.

42. Hillas, A.M. The origin of ultra-high energy cosmic rays. *Annu. Rev. Astron. Astrophys.* **1984**, *22*, 425–444. [CrossRef]

43. Kotera, K.; Olinto, A.V. The astrophysics of ultrahigh energy cosmic rays. *Ann. Rev. Astron. Astrophys.* **2011**, *49*, 119–153. [CrossRef]

44. de Jager, O.C.; Meintjes, P.J.; O' Donoghue, D.; Robinson, E.L. The discovery of a brake on the white dwarf in AE Aquarii. *Mon. Not. R. Astron. Soc.* **1994**, *267*, 577–588. [CrossRef]

45. Becker, W.; Trümper, J. The X-ray luminosity of rotation powered neutron stars. *Astron. Astrophys.* **1997**, *326*, 682–691.

46. Li, X.-H.; Lu, F.-J.; Lu, Z. Nonthermal X-ray properties of rotation powered pulsars and their wind nebulae. *Astrophys. J.* **2008**, *682*, 1166–1176. [CrossRef]

47. Eracleous, M.; Horne, K. A speedy magnetic propeller in in the cataclysmic variable AE Aquarii. *Astrophys. J.* **1996**, *471*, 427–446. [CrossRef]

48. Wynn, G.A.; King, A.R.; Horne, K. A magnetic propeller in the magnetic cataclysmic variable AE Aquarii. *Mon. Not. R. Astron. Soc.* **1997**, *286*, 436–446. [CrossRef]

49. Meintjes, P.J.; de Jager, O.C. Propeller spin-down and the non-thermal emission from AE Aquarii. *Mon. Not. R. Astron. Soc.* **2000**, *311*, 611–620. [CrossRef]

50. Ikhsanov, N.R.; Neustroev, V.V.; Beskrovnaya, V.V. On the mass transfer in AE Aquarii. *Astron. Astrophys.* **2004**, *421*, 1131–1142. [CrossRef]

51. Meintjes, P.J.; Venter, L.A. The diamagnetic blob propeller in AE Aquarii and non-thermal radio to mid-infrared emission. *Mon. Not. R. Astron. Soc.* **2005**, *360*, 573–582. [CrossRef]

52. Goldreich, P.; Julian, W.H. Pulsar electrodynamics. *Astrophys. J.* **1965**, *157*, 869–880. [CrossRef]

53. Sturrock, P.A. A model of pulsars. *Astrophys. J.* **1971**, *164*, 529–556. [CrossRef]

54. Cheng, K.A.; Ho, C.; Ruderman, M. Energetic radiation from rapidly spinning pulsars. I Outer Magnetospheric Gaps. *Astrophys. J.* **1986**, *300*, 500–521. [CrossRef]

55. Arons, J.; Scharlemann, E.T. Pair formation above pulsar polar caps:Structure of the low-altitude accelerator zone. *Astrophys. J.* **1979**, *231*, 854–879. [CrossRef]

56. Ikhsanov, N.R.; Biermann, P. High energy emission from fast rotating white dwarfs. *Astron. Astrophys.* **2006**, *445*, 305–312. [CrossRef]

57. Oruru, B.; Meintjes, P.J. X-ray characteristics and the spectral energy distribution of AE Aquarii. *Mon. Not. R. Astron. Soc.* **2012**, *421*, 1557–1568. [CrossRef]

58. Meintjes, P.J. The Propeller white dwarf in AE Aquarii: A Multi-Frequency Emission Laboratory. In Proceedings of the Golden Age of Cataclysmic Variables and Related Objects Workshop III, Palermo, Italy, 7–12 September 2015.

59. Meintjes, P.J. Magnetically driven transient phenomena in accretion driven systems: New breakthroughs with meerKAT and CTA? In Proceedings of the Accretion Processes in Cosmic Sources (APCS2016), Saint Petersburg, Russia, 5–10 September 2016.

60. Meintjes, P.J. On the multi-frequency emission and evolution of the white dwarfs binary system AR Scorpii. In Proceedings of the XII Multifrequency Behaviour of High Energy Cosmic Sources Workshop, Palermo, Italy, 12–17 June 2017.

61. Ghisellini, G. *Radiative Processes in High Energy Astrophysics*; Lecture Notes in Physics 873 (2013th edition); Springer: Berlin, Germany, 2013.

62. Erber, T. High-Energy Electromagnetic Conversion Processes in Intense Magnetic Fields. *Rev. Mod. Phys.* **1966**, *38*, 626–659. [CrossRef]

63. Zhang, B.; Gil, J. GCRT J1745-3009 As a transient white dwarf pulsar. *Astrophys. J.* **2005**, *631*, L143–L146. [CrossRef]

64. Ruderman, M.A.; Sutherl, P.G. Theory of pulsars: Polar gaps, sparks, and coherent microwave radiation. *Astrophys. J.* **1975**, *196*, 51–72. [CrossRef]

65. Chen, K.; Ruderman, M. Pulsar death lines and death valley. *Astrophys. J.* **1993**, *402*, 264–270. [CrossRef]

66. Zhang, B.; Harding, A. Full polar cap cascade scenario: Gamma-ray and X-ray luminosities from spin-powered pulsars. *Astrophys. J.* **2000**, *532*, 1150–1171. [CrossRef]

67. Harding, A.K.; Muslimov, A.G.; Zhang, B. Regimes of pulsar pair formation and particle energetics. *Astrophys. J.* **2002**, *576*, 366–375. [CrossRef]

68. Cáceres, D.L.; de Carvalho, S.M.; Coelho, J.G.; de Lima, R.C.R.; Rueda, J.A. Thermal X-ray emission from massive, fast rotating, highly magnetized white dwarfs. *Mon. Not. R. Astron. Soc.* **2017**, *465*, 4434–4440. [CrossRef]

69. Madzime, S.T.; Meintjes, P.J.; van Heerden, H.J.; Singh, K.K.; Buckley, D.A.H.; Woudt, P.A.; Fender, R. The detection of pulsed emission at the spin-period of the white dwarf in AE Aquarii in MeerKAT and Fermi-LAT data. In Proceedings of the 8th High Energy Astrophysics in Southern Africa (HEASA2021) Conference, Online, 13–17 September 2021.

70. Madzime, S.T. The Search for Pulsed Radio and Gamma-ray Emission from the Cataclysmic Variable System AE Aquarii Using MeerKAT and Fermi-LAT Data. Master's Dissertation, University of the Free State, Bloemfontein, South Africa, December 2021. [CrossRef]

71. Ochelkov, I.P.; Usov, V.V. Curvature radiation of relativistic particles in the magnetospheres of pulsars. *Astrophys. Space Sci.* **1980**, *69*, 439–460. [CrossRef]

72. Terada, Y.; Hayashi, T.; Ishida, M.; Mukai, K.; Dotani, T.; Okada, S.; Nakamura, R.; Naik, S.; Bamba, A.; Makishima, K. Suzaku discovery of hard X-ray pulsations from a rotating magnetized white dwarf, AE Aquarii. *Publ. Astron. Soc. Jpn.* **2008**, *60*, 387–397. [CrossRef]

73. Singh, K.K.; Meintjes, P.J.; Kaplan, Q.; Ramamonjisoa, F.A.; Sahayanathan, S. Modelling the broadband emission from the white dwarf binary system AR Scorpii. *Astropart. Phys.* **2020**, *123*, 102488. [CrossRef]

74. Li, J.; Torres, D.F.; Rea, N.; de Oña Wilhelmi, E.; Papitto, A.; Hou, X.; Mauche, C.W. Search for gamma-ray emission from AE Aquarii with seven years of Fermi-LAT data. *Astrophys. J.* **2016**, *832*, 35. [CrossRef]

75. Mattox, J.R.; Bertsch, D.L.; Chiang, J.; Dingus, B.L.; Digel, S.W.; Esposito, J.A.; Fierro, J.M.; Hartman, R.C.; Hunter, S.D.; Kanbach, G.; et al. The likelihood analysis of EGRET data. *Astrophys. J.* **1996**, *461*, 396–407. [CrossRef]

76. Mardia, K. *Statistics of Directional Data*; Academic Press: New York, NY, USA, 1972.

77. Kaplan, Q. The Search for High-Energy Gamma-ray Emission from the Close Binary System AR Scorpii Using Fermi-LAT Data. Master's Dissertation, University of the Free State, Bloemfontein, South Africa, April 2022. [CrossRef]

78. Kaplan, Q.; Meintjes, P.J.; van Heerden, H.J. Low-power pulsed emission at the spin period of the white dwarf in AR Scorpii? In Proceedings of the 8th High Energy Astrophysics in Southern Africa (HEASA2021) Conference, Online, 13–17 September 2021.

79. Funk, S.; Hinton, J.A.; The CTA Consortium 2013. Comparison of Fermi-LAT and CTA. *Astropart. Phys.* **2018**, *43*, 348–355. [CrossRef]
80. Bianco, F.B.; Ivezić, Ž.; Jones, R.L.; Graham, M.L.; Marshall, P.; Saha, A.; Strauss, M.A.; Yoachim, P.; Ribeiro, T.; Anguita, T.; et al. Optimization of the observing cadence for the Vera Rubin Observatory Legacy Survey of Space and time: A Pioneering Process of community-focused experimental design. *Astrophys. J. Suppl. Ser.* **2022**, *258*, 1. [CrossRef]